

# Geometrical locus of massive test particle orbits in the space of physical parameters in Kerr space-time.

F. Fayos\*, Ch. Teijón

Department of Applied Physics, UPC, Barcelona, Spain.

## Abstract

Gravitational radiation of binary systems can be studied by using the adiabatic approximation in General Relativity. In this approach a small astrophysical object follows a trajectory consisting of a chained series of bounded geodesics (orbits) in the outer region of a Kerr Black Hole, representing the space time created by a bigger object. In our paper we study the entire class of orbits, both of constant radius (spherical orbits), as well as non-null eccentricity orbits, showing a number of properties on the physical parameters and trajectories. The main result is the determination of the geometrical locus of all the orbits in the space of physical parameters in Kerr space-time. This becomes a powerful tool to know if different orbits can be connected by a continuous change of their physical parameters. A discussion on the influence of different values of the angular momentum of the hole is given. Main results have been obtained by analytical methods.

PACS numbers: 0420q, 0430D, 0470B

## 1 Introduction

Orbits (geodesics with null or non null eccentricity) in the outer region of Kerr space time play an important role in the description of important astrophysical phenomena near black holes. This space-time, characterized by the parameters  $M$  and  $a$  interpreted as the mass and angular momentum per unit of mass of a rotating hole, can be described in the outer region (limited by the outer horizon and the asymptotically flat region) by the Boyer-Linquist coordinate  $x^\alpha \equiv \{t, r, \theta, \phi\}$ .

Geodesics are characterized by four constants of motion, that are  $E, m, L$  and  $\mathcal{L}$ , representing, respectively, the energy as measured by an observer at infinity, the mass of a test particle, the component of the angular momentum along the axis of symmetry, and the Carter's constant, that can be interpreted as the parallel component of the four momentum when the particle crosses the equatorial plane of the hole. Sometimes, it will be interesting to use  $Q$  instead  $\mathcal{L}$ , where  $Q = p_\alpha p_\beta K^{\alpha\beta} \geq 0$ , where  $\mathbf{K}$  is the conformal Killing tensor of the Kerr space-time and  $p^\alpha \equiv dx^\alpha/d\lambda$  is the four momentum of the test particle (remember that  $Q = \mathcal{L} + (L - aE)^2$ ).

---

\*Also at Laboratori de Física Matemàtica, Societat Catalana de Física, IEC, Barcelona.

An extended summary of geodesics in Kerr space time can be found in the well known Chandrasekhar book "The mathematical theory of black holes" (1983) [7]. The algebraic complexity of the geodesic equation limited the analytical analysis to particular cases (geodesics in the equatorial plane, in the extreme Kerr geometry  $a = M$ , etc.). More recently E.Teo [8] studied spherical light rays out of equatorial plane finding an analytical expression for the amount of azimuth for a complete latitudinal oscillation of a spherical orbit (the Wilkins effect). This work extends an early result of D.C. Wilkins [9] devoted to particle spherical orbits in  $a = M$  case.

More recently, Drasco and Hughes [4] have studied the fundamental orbital frequencies in the " $r$ ", " $\theta$ " and " $\phi$ " motion of a test particle using Mino time [2]. This work improves an elegant proposal of Schmidt [5], based on the "action angle variables" formalism [6].

During the last decade, several works have been devoted to the study of one of the most important problems in gravitation, where geodesics play an important role, that is, to compute, according to the General Relativity, the gravitational radiation that one can expect from different astronomical sources. One kind of these sources are the so called extreme mass ratio inspiral, EMRI's: These binary systems are formed as a result of the capture of a compact stellar remnants by supermassive black holes in the nuclei of galaxies. The dynamics of such systems are (almost) purely gravitational, accurately modeled as a point particle of mass  $m$ , representing the star, following a trajectory in the background space-time created by a Kerr Black Hole. If the ratio  $m/M$  is infinitesimal the particle moves along a geodesic. In this system, the particle, having a finite mass, radiates gravitational waves. In such a case the trajectory deviates from a geodesic, but as the time scale of the orbital evolution is notably smaller than the typical time scale of orbits, the particle (approximately) slowly passes from one geodesic to another, conforming the so called "adiabatic approximation". Then, radiation reaction effect is characterized by the time evolution of the parameters  $E, L, Q$  of orbits.

In order to compute this time evolution of parameters different approaches have been built: using of post Newtonian methods, conservation laws, direct computation of self-force and time-domain numerical simulations. See for example, among others: Sago and alt.[3] which have obtained an analytic formulae for the change rates of the energy, angular momentum (using balance argument) and Carter constant (based partially on a Mino proposal [2] using the radiative field) (see references therein), or S. Drasco and S.A. Hughes [1], that have recently studied the gravitational wave snapshots of generic extreme mass ratio inspirals, or the 2007 work "Improved approximated inspirals of test-bodies into Kerr black holes" of Gair and Glampedakis [16], etc. .

In all these papers adiabatic approximation is implemented, and thus, an accurately knowledge of orbits in Kerr black hole is needed. As an interesting example, we focus on the work of different authors that have contributed to the study of the gravitational radiation effect on the spherical orbits showing that one spherical orbit remains spherical after radiation in the adiabatic approximation (see [10], [12],[11], etc.).

In this context, our main goal is to carry out an exhaustive analysis of orbits of test particle in the outer region of the Kerr space-time improving our theoretical knowledge, but trying to show how one orbit is related to each other, in other words, if they can connect through a continuous change of parameters. We extend the analytical results on the equatorial plane to the whole

outer region finding the set of values that constants of motion can reach and showing the range of coordinates that we expect for an allowed set of constants of motions of physical null and non-null eccentricity orbits. This analysis allow us to have a global view of all orbits that we show in a formal three-dimensional (normalized) parameters space ,  $\hat{Q}$ ,  $\hat{L}$ , and  $\hat{E}$ , where

$$\hat{Q} \equiv \frac{Q}{m^2 M^2}, \quad \hat{L} \equiv \frac{L}{mM}, \quad \hat{E} \equiv \frac{E}{m}. \quad (1)$$

In this parameter space each orbit is represented by a point. The whole set of orbits is confined in a compact volume (see figure (6) that partially diverge when  $\hat{E} \rightarrow 1$  and vanishes when  $\hat{E} < z_a^{-1/2}$  (see equation (62) for  $z_{a,b}$  definitions). Spherical orbits are represented by an upper face (stable) and a lower one (unstable). Slices of this volume with  $\hat{E} = \text{constant}$  come first ( $\hat{E}$  slightly less than 1 ) a pseudo-rectangle (upper side to stable, lower side to unstable, the two bases for orbits on the equatorial plane) , and after ( $z_a^{-1/2} < \hat{E} \leq z_b^{-1/2}$ ) a pseudo-triangle( the two sides of spherical orbits joints in one vertex when  $z = z_b$  see (62)) showing that this triangle vanishes when  $\hat{E} < z_a^{-1/2}$  (see section 4). This representation in the space of parameters allow us to study the different paths that a particle can follow going through different geodesics after a continuous change of constants of motion. As an specific application, we obtain the necessary and sufficient condition that evolving parameters have to accomplish to go from one spherical geodesic to another, showing its limits of application. This result can also be found in [10] and [12] in different scenarios and using different techniques.

In section II, III and IV we analyze the geodesics out of the equatorial plane in Kerr space time using well known results in literature [7],[9],[8]. In section V and VI we construct the abstract 3-space of parameters showing the geometrical locus of spherical and non null eccentricity orbits in that space, respectively. Some proofs can be find in Appendices I and II.

### First order differential equations for geodesic motion of massive particles.

Using the Hamilton-Jacobi method, Carter found the equations of motion for test particles (see for example [15]). In the Boyer-Linquist coordinates these equations are

$$\rho^2 \frac{dr}{d\lambda} = \pm \{[(r^2 + a^2)E - aL]^2 - \Delta[m^2 r^2 + (L - aE)^2 + \mathcal{L}]\}^{1/2} \quad (2)$$

$$\rho^2 \frac{d\theta}{d\lambda} = \pm \{\mathcal{L} - [(m^2 - E^2)a^2 + \frac{L^2}{\sin^2 \theta}]\cos^2 \theta\}^{1/2} \quad (3)$$

$$\rho^2 \frac{d\phi}{d\lambda} = -(aE - \frac{L}{\sin^2 \theta}) + \frac{a[E(r^2 + a^2) - aL]}{\Delta} \quad (4)$$

$$\rho^2 \frac{dt}{d\lambda} = -a(aE \sin^2 \theta - L) + \frac{(r^2 + a^2)[E(r^2 + a^2) - aL]}{\Delta}. \quad (5)$$

where

$$\rho^2 = r^2 + a^2 \cos^2 \theta, \quad (6)$$

$$\Delta = r^2 - 2Mr + a^2 \equiv (r - r_+)(r - r_-), \quad (7)$$

$$r_{\pm} = M \pm \sqrt{M^2 - a^2}, \quad 0 \leq r_- \leq M \leq r_+ \leq 2M. \quad (8)$$

Without loss of generality, in the intermediate computations we are going to work with the

following dimensionless constants of motion, often used in the literature (see for example [7]):

$$\eta = \frac{\hat{\mathcal{L}}}{\hat{E}^2}, \quad \xi = \frac{\hat{L}}{\hat{E}}, \quad z = \frac{1}{\hat{E}^2}; \quad (9)$$

where  $\hat{\mathcal{L}} = \mathcal{L}/m^2M^2$ , considering that  $z = 0$  for photons, and  $z > 0$  for massive particles. In some cases, results exhibit a simpler form in terms of

$$\mathcal{Q} \equiv \hat{Q}/\hat{E}^2, \quad (10)$$

instead of  $\eta$ . We have to remember that, according with this definition,

$$\eta = \mathcal{Q} - (\xi - a)^2. \quad (11)$$

Replacing these three quantities in the equations of motion and taking into account that for massive particles  $\lambda = \tau/m$ , where  $\tau$  is the proper time, the equations become

$$\bar{\rho}^2 \frac{dx}{d\bar{\tau}} = \pm z^{-\frac{1}{2}} \sqrt{R} \quad (12)$$

$$\bar{\rho}^2 \frac{d\mu}{d\bar{\tau}} = \pm 2z^{-\frac{1}{2}} \sqrt{\Theta} \quad (13)$$

$$\bar{\rho}^2 \frac{d\phi}{d\bar{\tau}} = 2z^{-\frac{1}{2}} \left[ \left( \frac{1}{1-\mu^2} - \frac{\bar{a}^2}{\bar{\Delta}} \right) \xi + \frac{4\bar{a}x}{\bar{\Delta}} \right] \quad (14)$$

$$\bar{\rho}^2 \frac{d\bar{t}}{d\bar{\tau}} = z^{-\frac{1}{2}} \left\{ \bar{a}[\xi - \bar{a}(1-\mu^2)] + \frac{(4x^2 + \bar{a}^2)(4x^2 + \bar{a}^2 - \bar{a}\xi)}{\bar{\Delta}} \right\}. \quad (15)$$

where

$$R = -x(x-1)\left(\xi + \frac{a}{x-1}\right)^2 - \frac{\Delta}{4} \left\{ \eta - \frac{4x^2}{x-1} [z - (z-1)x] \right\} \quad (16)$$

$$\Theta = (1-\mu^2)\eta - \mu^2\xi^2 - \mu^2\bar{a}^2(z-1)(1-\mu^2), \quad (17)$$

$$\bar{\rho}^2 = 4x^2 + \bar{a}^2\mu^2 \quad (18)$$

$$\bar{\Delta} = 4x^2 - 4x + \bar{a}^2 \quad (19)$$

$$x = \frac{r}{2M}, \quad \mu = \cos\theta, \quad \bar{t} = \frac{t}{2M}, \quad \bar{\tau} = \frac{\tau}{2M}. \quad (20)$$

The allowed values of the independent constants of motion  $\xi, \eta$  and  $z$  are only limited by conditions  $R \geq 0$  and  $\Theta \geq 0$ . Equations (14) and (15) give us the variation of  $\phi$  and  $\bar{t}$  on proper time, once we have chosen allowed values of these constants.

From now on we will drop the bar symbol from  $\bar{a}$ ,  $\bar{\Delta}$  and  $\bar{\rho}$  considering that we will ever work with non-dimensional quantities.

As it is well known, these equations of motion are valid for all values of  $a$ . However, in our work we have differentiated  $a = 0$  case (The Schwarzschild space-time) from the  $0 < a \leq 1$  case.

Furthermore, we are interested in the bound geodesics ( $z > 1$ ) in the outer space-time of the hole, that is,  $x_+ \leq x \leq \infty$ .

## 2 Theta-motion for bound orbits

It is well known that, without loss of generality, we can study all geodesics in Schwarzschild ( $a = 0$ ) space-time in the equatorial plane ( $\theta = \pi/2$ ,  $d\theta/d\tau = 0$ ,  $\eta = 0$ ).

In order to analyze the whole set of geodesics in Kerr space-time  $0 < a \leq 0$ , the  $\theta$ -motion equation sets important restrictions on the  $\xi$  and  $\eta$  values.

Considering  $z \geq 1$  case (we include  $z = 1$  as a special case) condition  $\Theta \geq 0$  holds if and only if [7]

$$\eta \geq 0, \quad (21)$$

$$-\mu_- \leq \mu \leq \mu_-, \quad (22)$$

in accordance with (17), where

$$\mu_-^2 = \frac{1}{2\alpha^2} \{ \xi^2 + \eta + \alpha^2 - \sqrt{(\xi^2 + \eta + \alpha^2)^2 - 4\alpha^2\eta} \} \quad (23)$$

$$= \frac{1}{2\alpha^2} \{ \xi^2 + \eta + \alpha^2 - \sqrt{\xi^4 + (\eta - \alpha^2)^2 + 2\xi^2(\eta + \alpha^2)} \},$$

$$0 \leq \mu_-^2 \leq 1,$$

$$\alpha^2 = (z - 1)a^2,$$

$$\mu_- \equiv +\sqrt{\mu_-^2}. \quad (24)$$

In the  $z = 1$  case we find that if  $\eta = 0$ , then  $\mu = 0$  ( $\theta = \pi/2$ ) or  $\xi = 0$  and  $0 \leq \mu^2 \leq 1$ . Moreover, if  $\eta > 0$  geodesics may be found.

In the  $z > 1$  case,  $\eta = 0 \Rightarrow \mu^2(\xi^2 + \alpha^2(1 - \mu^2)) = 0$ . It implies:  $\mu^2 = 0 \Rightarrow \theta = \frac{\pi}{2}$ , or  $\xi^2 + \alpha^2(1 - \mu^2) = 0 \Rightarrow \xi = 0$  and  $\theta = 0, \pi$ . Besides, if  $\eta > 0$  geodesics exist.

According to (23),  $|\mu_-| = 1$ , if and only if  $\xi = 0$  and  $\eta > \alpha^2$ . It means that only the trajectories with  $\xi = 0$  can reach  $\theta = 0, \pi$ , that is, the symmetry axis. This result can be found not only in particle geodesics case but also in light rays geodesics (see [8]).

### 3 Locally Nonrotating Frame

There's a condition that arises when we consider that the photon's or particle's energy measured by any inertial observer cannot be negative or zero. We know that if one inertial frame measures positive energy then all inertial frames must measure positive energy. We will use an observer who, in some sense, rotates with the geometry, the so called 'locally nonrotating frames LNRF' (see [13] for definitions). Thus the observer world line is  $r = \text{constant}, \theta = \text{constant}, \phi = \omega t + \text{constant}$  where  $\omega = -g_{\phi t}/g_{\phi\phi}$ . The orthonormal tetrad carried by this observer is

$$\begin{aligned} \mathbf{e}_t &= \left(\frac{A}{\rho^2\Delta}\right)^{1/2} \frac{\partial}{\partial t} + \frac{2Mar}{(A\rho^2\Delta)^{1/2}} \frac{\partial}{\partial \phi}, & \mathbf{e}_r &= \left(\frac{\Delta}{\rho^2}\right)^{1/2} \frac{\partial}{\partial r}, & \mathbf{e}_\theta &= \left(\frac{1}{\rho^2}\right)^{1/2} \frac{\partial}{\partial \theta}, & \mathbf{e}_\phi &= \left(\frac{\rho^2}{\Delta \sin^2 \theta}\right)^{1/2} \frac{\partial}{\partial \phi}. \\ A &= (r^2 + a^2)^2 - a^2\Delta \sin^2 \theta. \end{aligned} \quad (25)$$

In this frame the measured energy is

$$E_{LNRF} = -p^\alpha \mathbf{e}_{t\alpha} = B^2(E - MwL), \quad (26)$$

where  $B$  is a non-diverging function and  $\omega$  is

$$w \equiv -\frac{g_{\phi t}}{g_{\phi\phi}} = \frac{4xa}{M[(4x^2 + a^2)^2 - a^2\Delta \sin^2 \theta]}. \quad (27)$$

It will be interesting to find bounds on  $\frac{1}{Mw}$ . These are

$$\frac{1}{Mw_m} \geq \frac{1}{Mw} \geq \frac{1}{Mw_M} > 0. \quad (28)$$

where

$$w_M \equiv \frac{4ax}{M(4x^2 + a^2)^2}$$

$$w_m \equiv \frac{a}{M[4x^3 + a^2(x+1)]}.$$

It is important to remark that

$$w_M(x_+) = w_m(x_+) = \frac{a}{2M(1 + \sqrt{1 - a^2})} > 0. \quad (29)$$

The requirement  $E_{LNRF} \geq 0$  is equivalent to  $E - MwL \geq 0$ . Therefore

$$\begin{aligned} E > 0 &\Rightarrow \xi \leq \frac{1}{Mw} \leq \frac{1}{Mw_m}, \\ E < 0 &\Rightarrow \xi \geq \frac{1}{Mw} \geq \frac{1}{Mw_M} > 0 \Rightarrow L < 0. \end{aligned} \quad (30)$$

In order to apply this rule out of the equatorial plane, ( $\eta \neq 0$ ), we use the relation (28) showing that  $\frac{1}{Mw}$  takes values bounded by two  $\theta$ -non-depending limits.

In the Schwarzschild case  $\omega = 0$  and then  $E_{LNRF} \geq 0 \Leftrightarrow E \geq 0$ .

## 4 Spherical orbits

Orbits with constant Boyer-Linquist coordinate “ $r$ ” ( $x = \text{constant}$ ) require that  $R = 0$ , and  $R' = 0$ , where  $R' = dR/dx$ . In the literature one refers to these orbits as ‘spherical’ or ‘circular’ orbits indistinctly. The analysis of spherical geodesics establishes a basis to classify the whole set of geodesics. We focus our work on the outer region of Kerr space-time  $x_+ \leq x$ , as we have said before.

Solving simultaneously  $R = 0$  and  $R' = 0$  equations we obtain general expressions for  $\xi_s$  and  $\eta_s$ , in terms of  $x_s$ , where  $a$  and  $z$  are taken as parameters (the subscript  $s$  means that these values correspond to spherical orbits). The solutions for  $\xi_s$  are

$$\xi_{s1,2} = \frac{4x_s^2 - a^2 \pm \Delta_s \sqrt{2x_s} \sqrt{2(1-z)x_s + z}}{(2x_s - 1)a}, \quad (31)$$

while the corresponding solutions for  $\eta_s$  are

$$\begin{aligned} \eta_{s1,2} = & \frac{4x_s^2}{(2x_s - 1)^2 a^2} \left[ z(2x_s - 1)(8x_s^3 - 16x_s^2 + 8x_s - a^2) - \right. \\ & \left. - 4x_s(4x_s^3 - 8x_s^2 + 5x_s - a^2) \mp 2\Delta_s \sqrt{2x_s} \sqrt{2(1-z)x_s + z} \right]. \end{aligned} \quad (32)$$

If  $1 < z$ , the necessary and sufficient condition for these solutions to exist is:

$$x_s \leq x_{s_{max}} \equiv \frac{z}{2(z-1)}. \quad (33)$$

Note that  $x_{s_{max}}$  is an upper bound to the radius of spherical orbit. This limit is independent of  $a$ , as long as  $a \neq 0$ .

From now on, we will focus on the following intervals for  $x$ ,  $a$  and  $z$ :  $x_+ \leq x \leq x_{s_{max}}$ ,  $1 \leq z$ ,  $0 < a \leq 1$  that we will generically call  $\mathcal{D}$ , the domain of variation of these quantities.

In order to ensure the existence of  $\mathcal{D}$  it is necessary that  $x_+ \leq x_{s_{max}}$ . This implies an upper bound of  $z$ , that is

$$1 \leq z \leq z_{s_{max}}, \quad (34)$$

where

$$z_{s_{max}} \equiv 1 + \frac{1}{\sqrt{1-a^2}}, \quad (35)$$

( $a = 0, z_{s_{max}} = 2$ ;  $a = 0.8, z_{s_{max}} = 2.66..$ ;  $a \rightarrow 1, z_{s_{max}} \rightarrow \infty$ ).

If  $1 \leq z$ , the  $\theta$ -motion analysis has shown that only non negative values of  $\eta$  need to be considered. Then circular orbits occur when  $\eta_{s1,2} \geq 0$ .

After a tedious calculus we can see that

$$\eta_{s1}(x_s, a, z) < 0 \quad (36)$$

in  $\mathcal{D}$  (see Appendix I). Therefore spherical orbits in Kerr space-time ( $0 < a \leq 1$ ) can be found if and only if  $\eta_{s2} \geq 0$ .

**A. The  $\{\eta_{s2}, \xi_{s2}\}$  solution.**

Firstly, we apply the results of section 3 to this solution. We can check that

$$\xi_{s2} \leq \frac{1}{M\omega_M} \leq \frac{1}{M\omega_m}, \quad (37)$$

(if  $x = x_+$  we get the equality). Therefore, according to (30): No spherical orbits exist if  $E < 0$  and all spherical orbits with  $E > 0$  have  $E_{LNRF} > 0$ .

The analytical complexity of these functions doesn't allow us to have a complete knowledge of them in a direct way. While  $\eta_{s2}$  has three extrema in  $\mathcal{D}$  (every extremum is a maximum, minimum or inflection point depending on the  $a$  and  $z$  values),  $\mathcal{Q}_{s2}$ , defined in (11),

$$\mathcal{Q}_{s2} = \eta_{s2} + (a - \xi_{s2})^2 \quad (38)$$

only has one and shows other interesting properties that we will discuss below.

The function  $R$  can be written as follows

$$R = A(\xi + B)^2 + C(\mathcal{Q} + g), \quad (39)$$

where  $A, B, C, g$  are

$$A = \frac{a^2}{4}, \quad B(x, a) = -\frac{4x^2 + a^2}{a}, \quad C(x, a) = -\frac{\Delta}{4}, \quad g(x, z) = 4zx^2. \quad (40)$$

Thus  $R$  must be considered as a function of  $x, a, C^i$ , i.e.  $R(x, a, C^i)$ , where  $C^i \equiv \{\xi, \mathcal{Q}, z\}$ . According to this we define

$$R' \equiv \frac{\partial R}{\partial x}, \quad R'' \equiv \frac{\partial R'}{\partial x} \quad (41)$$

$$B' \equiv \frac{dB}{dx}, \quad C' \equiv \frac{dC}{dx}, \quad g' \equiv \frac{dg}{dx}. \quad (42)$$

For each set of allowed values of  $C^i$  we can find a solution  $x = x(\tau, C^i, a)$  solving equation (12). Thus  $R = R(x(\tau, C^i, a), C^j, a)$ .

We are now interested in a family of solutions such that the parameters vary according to a specific law, defined by the functions  $C^i(s)$ , assuming that for each value of  $s$  we obtain a geodesic [12]. The solution of (12) now takes the form  $x = x(\tau, C^i(s), a)$ , and thus

$$R = R(x(\tau, C^i(s), a), C^j(s), a). \quad (43)$$

If we produce a small variation  $\delta s$  then the quantities  $R$  and  $R'$  vary according to

$$\frac{\delta R}{\delta s} = R' \dot{x} + \sum_{i=1,3} \frac{\partial R}{\partial C^i} \dot{C}^i \quad (44)$$

$$\frac{\delta R'}{\delta s} = R'' \dot{x} + \sum_{i=1,3} \frac{\partial R'}{\partial C^i} \dot{C}^i. \quad (45)$$

where  $\dot{x} \equiv \partial x / \partial s$  and  $\dot{C}^i \equiv \partial C^i / \partial s$ .

We apply this results in order to investigate the properties of the first derivatives of  $\xi_{s2}(x_s, a, z)$  and  $\mathcal{Q}_{s2}(x_s, a, z)$ .

Spherical orbits imply  $x = s \equiv x_s$ . This means  $\dot{x} = 1$ , thus,  $\xi(s \equiv x_s) = \xi_{s2}(x_s, z, a)$ ,  $\mathcal{Q}(s \equiv x_s) = \mathcal{Q}_{s2}(x_s, z, a) = \eta_{s2}(x_s, z, a) + (a - \xi_{s2}(x_s, z, a))^2$  and  $\dot{z} = 0$ . For every allowed value of  $s \equiv x_s$  we have spherical orbits, therefore  $R(x_s, \xi_{s2}, \mathcal{Q}_{s2}, z, a) = R'(x_s, \xi_{s2}, \mathcal{Q}_{s2}, z, a) = 0$ . As we go from one spherical orbit to another varying  $s$ , hence  $\dot{R}(x_s, \xi_{s2}, \eta_{s2}, z, a) = \dot{R}'(x_s, \xi_{s2}, \eta_{s2}, z, a) = 0$ . Using these results on (41), (44) and (45) we obtain

$$0 = 2A(\xi_{s2} + B_s)B'_s + C'_s(\mathcal{Q}_{s2} + g_s) + C_s g'_s, \quad (46)$$

$$0 = 2A(\xi_{s2} + B_s)\xi'_{s2} + C_s \mathcal{Q}'_{s2} \quad (47)$$

$$0 = R''_s + 2AB'_s \xi'_{s2} + C'_s \mathcal{Q}'_{s2}, \quad (48)$$

where for example  $B_s \equiv B(x = x_s)$ , and  $\dot{\xi}_{s2} \equiv \partial \xi_{s2} / \partial x_s \equiv \xi'_{s2}$ , in accordance with our previous notation.

**Theorem I:**  $\xi'_s(x_e(a, z), a, z) = 0$  if and only if  $\mathcal{Q}'_s(x_e(a, z), a, z) = 0$ , where  $x_s = x_e(z, a)$  is a solution of  $\xi'_s(x_s, a, z) = \mathcal{Q}'_s(x_e(a, z), a, z) = 0$ . In other words, there where  $\xi_s(x_s, a, z)$  has an extremum, the function  $\mathcal{Q}_s(x_s, a, z)$  must have an extremum, and vice versa.

Proof: Considering that  $\xi_{s2}$  and  $\mathcal{Q}_{s2}$  satisfy  $R'(\xi_{s2}, \eta_{s2}, x_s, a, z) = 0$ , then, according to (47), if  $\xi'_{s2} = 0$  then  $\mathcal{Q}'_{s2} = 0$  since  $C_s = -\Delta_s/4 \leq 0$  ( $x_+ \leq x_s \leq x_{s_{max}}$ ). Conversely, if  $\mathcal{Q}'_{s2} = 0$  it implies that  $\xi'_{s2} = 0$  since the other possibility  $\xi_{s2} = -B_s$ ,  $g'_s = 0$  and  $\mathcal{Q}_{s2} = -g_s$  (to ensure  $R = R' = 0$ ) is impossible due to  $g_s > 0$  and  $\mathcal{Q}_{s2}$  must be greater than zero.

In Appendix III we have proved that this extremum exists and is unique. We call it  $x_e(a, z)$  but we are not able to found his analytical expression.

From equation  $\xi'_{s2} = 0$  we can obtain

$$z_e = \frac{8x_e}{(32x_e^3 - 36x_e^2 + 12x_e - a^2)^2} [2x_e(2x_e - 1)(32x_e^3 - 44x_e^2 + 20x_e - 3a^2) - \Delta_e^{\frac{3}{2}} \sqrt{2x_e}]. \quad (49)$$



Using this expression we find

$$\xi_{e2}(x_e, a) = \xi_{s2}(x_s = x_e, a, z = z_e) \quad (50)$$

$$\mathcal{Q}_{e2}(x_e, a) = \mathcal{Q}_{s2}(x_s = x_e, a, z = z_e). \quad (51)$$

where the functions  $\xi_{e2}(x_e, a)$ ,  $z_e(x_e, a)$  and  $\mathcal{Q}_{e2}(x_e, a)$  represent the values of minimum of  $\xi_{s2}$ , maximum of  $\mathcal{Q}_{s2}$  and  $z_e$  when the extremum is in  $x_e$ .

**Theorem II:** The function  $R''(\xi_{s2}, \mathcal{Q}_{s2}, x_s, a, z)$  vanishes if and only if  $\xi'_{s2}(x_s, a, z) = \mathcal{Q}'_{s2}(x_s, a, z) = 0$ .

Proof: The right to left implication is obvious using (48). The left to right implication can be proved considering that the determinant of unknowns  $\xi'_{s2}$  and  $\mathcal{Q}'_{s2}$  in the homogeneous system of two equations (47) and (48), considering that now  $R'' = 0$ , is

$$Det = 2A_s(\xi_{s2} + B_s)C'_s - 2A_sB'_sC_s = \frac{\Delta_s}{2}\sqrt{-2x_s(2x_s z - 2x_s - z)}. \quad (52)$$

It is clear that  $Det$  only vanishes in  $x = x_+$  and  $x = x_{s_{max}}$ . Then the only solution is  $\xi'_{s2}(x_s, a, z) = \mathcal{Q}'_{s2}(x_s, a, z) = 0$  in  $x_+ < x_s < x_{s_{max}}$ .

As it is well known stable (unstable) spherical orbits occur when  $R''(x, a, \mathcal{Q}_{s2}, \xi_{s2}, z) < 0 (> 0)$ .

Theorem II implies that  $R'' = 0$  only where  $\mathcal{Q}'_{s2}(x_s, a, z) = \xi'_{s2}(x_s, a, z) = 0$ , that is, where  $x = x_e(a, z)$ . It is not difficult to prove that spherical orbits are stable when  $x_s > x_e(a, z)$ . Conversely, if  $x_s < x_e$  they are unstable.

**Theorem III:** The extremum of  $\xi_{s2}$  and  $\mathcal{Q}_{s2}$  are maximum (minimum) and minimum (maximum) respectively in  $\mathcal{D}$ .

From (47), and considering the point where  $\xi'_{s2} = \mathcal{Q}'_{s2} = 0$  we obtain

$$\frac{\xi''_{s2}}{\mathcal{Q}''_{s2}} = -\frac{C_s}{2A_s(\xi_{s2} + B_s)} < 0. \quad (53)$$

Numerical calculations show that this point is always a maximum of  $\mathcal{Q}_{s2}$  and a minimum of  $\xi_{s2}$ .

The values of these two functions in  $x_+$  and  $x_{s_{max}}$  are

$$\begin{aligned} \mathcal{Q}_{s2}(x_+, a, z) &= -(1 + \sqrt{1 - a^2})z < 0, \\ \mathcal{Q}_{s2}(x_{s_{max}}, a, z) &= -\frac{z^2}{z - 1}[z(1 - a^2) + a^2] < 0, \\ \xi_{s2}(x_+, a, z) &= \frac{2(1 + \sqrt{1 - a^2})}{a} > 0, \\ \xi_{s2}(x_{s_{max}}, a, z) &= \frac{z}{a(z - 1)}[z(1 - a^2) + a^2] + a > 0. \end{aligned} \quad (54)$$

$$\xi_{s2}(x_{s_{max}}, a, z) = \frac{z}{a(z - 1)}[z(1 - a^2) + a^2] + a > 0. \quad (55)$$

**B**  $\xi_{s2} = \xi'_{s2} = 0$ .

It will be important to find the functions  $z_c(a)$  and  $x_{ec}(a)$  such that if  $z > z_c$  then  $\xi_{s2}(x_s, a, z) > 0$ , where  $x_{ec}$  is the point where  $\xi_{s2} = \xi'_{s2} = 0$ , for any value of  $a$ . To do this we proceed as follows: First, the system of equations  $\xi_{s2} = \xi'_{s2} = 0$  is equivalent to

$$a = 2x_{ec}^{1/2} \left[ -x_{ec} + 1 + \frac{1}{9} \left( A(x_{ec})^{1/3} - A(x_{ec})^{-1/3} + \sqrt{2} \right)^2 \right]^{1/2}, \quad (56)$$

$$z_c = \frac{1}{2} \frac{(4x_{ec}^2 + a^2)(8x_{ec}^3 - 12x_{ec}^2 + 2a^2x_{ec3c} + a^2)}{(4x_{ec}^2 - 4x_{ec3c} + a^2)^2 x_{ec}}, \quad (57)$$

where

$$A(x_{ec}) = 11\sqrt{2} - 27\sqrt{2}x_{ec} + 3\sqrt{27 - 132x_{ec} + 162x_{ec}^2}. \quad (58)$$

If we use (56) in (57) we obtain a function  $z_c(x_{ec})$  that combined with (56) is a parametric expression of  $z_c(a)$  (see figure (1),a), that is, for every  $a$  we find  $z_c$ . Then, using (58) (see figure (1), b) we can find  $x_{ec}$  value.

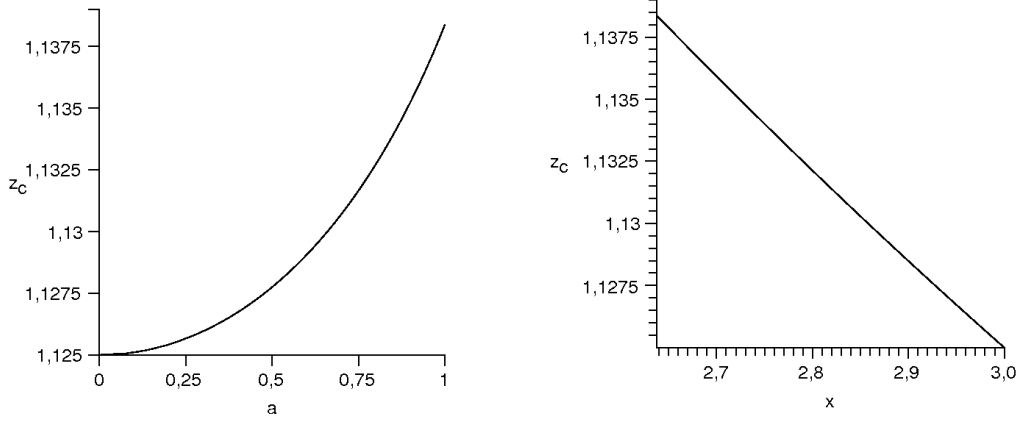


Figure 1: Plot of  $z_c(a)$  and  $z_c(x_{ec})$

Numerical examples can be done:  $a = 0, x_{ec} = 3, z_c = 1.125$ ;  $a = 0.8, x_{ec} = 2.784, z_c = 1.133$  and  $a = 1, x_{ec} = 2.637255281, z_c = 1.138373645$ .

As an interesting application of this result, we can prove that  $d\phi/d\tau \geq 0$  for all spherical orbits provided  $z \geq z_c$ . According to (14)

$$\frac{z^{\frac{1}{2}}\bar{\rho}^2}{2} \frac{d\phi}{d\bar{\tau}} = \left( \frac{1}{1-\mu^2} - \frac{a^2}{\Delta} \right) \xi_{s2} + \frac{4ax}{\Delta} \geq \left( 1 - \frac{a^2}{\Delta} \right) \xi_{s2} + \frac{4ax}{\Delta}. \quad (59)$$

But

$$\left( 1 - \frac{a^2}{\Delta} \right) \xi_{s2} + \frac{4ax}{\Delta} - \xi_{s2} = \frac{a \left( 1 + \sqrt{2} \sqrt{-(-2x + 2zx - z)x} \right)}{2x - 1} > 0. \quad (60)$$

Therefore

$$\frac{z^{\frac{1}{2}}\bar{\rho}^2}{2} \frac{d\phi}{d\bar{\tau}} = \left( \frac{1}{1-\mu^2} - \frac{a^2}{\Delta} \right) \xi_{s2} + \frac{4ax}{\Delta} > \xi_{s2}. \quad (61)$$

Thus, we can conclude that:

**Theorem IV.** For every value of  $a$ , there exists  $z_c$ , defined by (57) and (56), such that if  $z \geq z_c$  then  $\xi_{s2} \geq 0$  in  $\mathcal{D}$  and thus  $d\phi/d\tau > 0$ , i.e. the spherical orbits co rotate with the hole.

$$\mathbf{C} \mathcal{Q}_{s2} - (a - \xi_{s2})^2 = \mathcal{Q}'_{s2} - [(a - \xi_{s2})^2]' = 0.$$

In order to improve our knowledge of  $x_e$ , we can find where both  $\mathcal{Q}_{s2} = (a - \xi_{s2})^2$  and  $\mathcal{Q}'_{s2} = [(a - \xi_{s2})^2]' = 0$ , or alternatively  $\eta_{s2} = \eta'_{s2} = 0$ . These conditions are equivalent to

$$z_{a,b} = \frac{3x_{ea,b}}{3x_{ea,b} - 1}, \quad (62)$$

$$x_{ea,b} = \frac{1}{2} \{3 + Z_2 \mp [(3 - Z_1)(3 + Z_1 + 2Z_2)]^{\frac{1}{2}}\}. \quad (63)$$

where

$$\begin{aligned} Z_1 &= 1 + (1 - a^2)^{\frac{1}{3}} [(1 + a)^{\frac{1}{3}} + (1 - a)^{\frac{1}{3}}], \\ Z_2 &= (3a^2 + Z_1^2)^{\frac{1}{2}}. \end{aligned}$$

Functions  $x_{ea,b}$  were first presented in [13] (see equation (2.21) in that paper). We now show some values of these variables:

- When  $a = 1$  then  $z_a = 3$  and  $z_b = 1.080$  while  $x_{ea} = 1/2$  and  $x_{eb} = 9/2$ ,
- When  $a = 0.8$  then  $z_a = 1.298$  and  $z_b = 1.086$  while  $x_{ea} = 1.453$  and  $x_{eb} = 4.216$ ,
- When  $a \rightarrow 0$  then  $z_a, z_b \rightarrow 9/8$  while  $x_{ea}, x_{eb} \rightarrow 3$ .

Moreover,  $x_{ea,b}$  give us the range of variations of  $x_e$ , that is  $x_{eb}(a) \leq x_e(z, a) \leq x_{ea}(a)$  obtaining non-negative values of  $\eta_{s2}$ .

Finally, we can verify that  $1 < z_b < z_a$ , see fig (2).

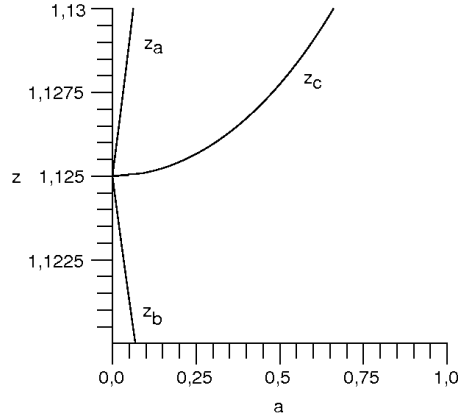


Figure 2: Dependence on  $a$  of  $z_b, z_c$  and  $z_a$ .

The behavior of these functions near  $a = 0_+$  is

$$\begin{aligned} z_b &= \frac{9}{8} - \frac{\sqrt{6}}{32}a + O(a^2) \\ z_c &= \frac{9}{8} + \frac{1}{48}a^2 + O(a^3) \\ z_a &= \frac{9}{8} + \frac{\sqrt{6}}{32}a + O(a^2). \end{aligned}$$

this implies that  $z_b \leq z_c \leq z_a$  (the equality holds in the limit  $a \rightarrow 0$ ).

**D Classification.**

Until now we have studied the functions  $Q_{s2}$  and  $\xi_{s2}$ . We conclude this subsection analyzing under which conditions  $Q_{s2} \geq (a - \xi_{s2})^2$  ( $\Leftrightarrow \eta_{s2} \geq 0$ ) holds. We call  $x_i, i, j, .. \equiv \{1, 2, \dots\}$ ,  $x_i \leq x_{i+1}$ , the points where  $Q_{s2} = (a - \xi_{s2})^2$ . We will depict these two functions  $Q_{s2}$  and  $(a - \xi_{s2})^2$  in four possible scenarios (see figure 3):

- I)  $1 < z < z_b$ . Condition only holds in two disconnected intervals,  $x_+ < x_1 \leq x \leq x_2 < x_e$  for the unstable spherical orbits (in which  $Q_{s2}$  is an increasing function) and  $x_e < x_3 \leq x \leq x_4 < x_{smax}$  that corresponds to the stable ones (in which  $Q_{s2}$  is a decreasing function),
- II)  $z = z_b$ . The two parts are just connected in  $x_e$ , that is  $x_2 = x_e = x_3$  of the previous case, and we can continuously go from the stable to the non-stable orbits,
- III)  $z_b < z < z_a$ . The condition holds in the whole interval  $x_+ < x_1 \leq x \leq x_4 < x_{smax}$  containing stable and unstable orbits (now  $x_2$  and  $x_3$  doesn't exist).
- IV)  $z = z_a$ . We only have one spherical geodesic in  $x_e$ .

In figure 4, we can see  $\xi_{s2}$  in these cases, including  $z = z_c$ .

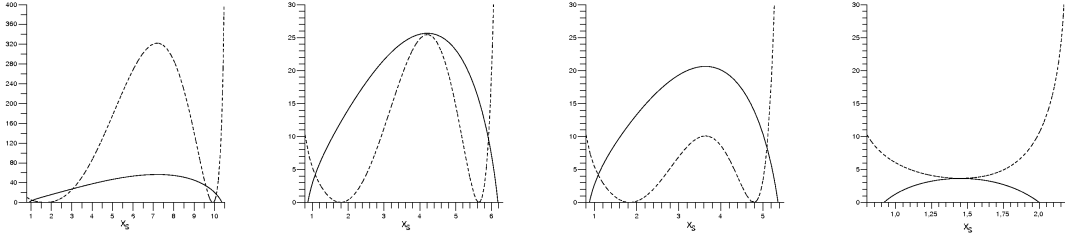


Figure 3: Plot of  $Q_{s2}$  (continuous line) and  $(a - \xi_{s2})^2$  (dashed line) corresponding to I; II; III; IV cases

**E Equatorial Plane.**

As it is well known, a necessary condition to have orbits lying entirely in the equatorial plane is  $\eta = Q - (\xi - a)^2 = 0$ . For spherical orbits the condition becomes  $\eta_{s2} = 0$ .

Conditions  $R = R' = 0$  are now ( $\eta = 0$ ) equivalent to

$$z_{s\pm} = 4 \frac{[16x_s^5 - 56x_s^4 + 64x_s^3 - 6(a^2 + 4)x_s^2 + 5a^2x_s \pm a\Delta_s\sqrt{2x_s}]x_s}{(8x_s^3 - 16x_s^2 + 8x_s - a^2)^2}$$

$$\xi_{s\pm} = \frac{-a(12x_s^2 - 8x_s + a^2) \mp 2\Delta_s x_s \sqrt{2x_s}}{8x_s^3 - 16x_s^2 + 8x_s - a^2} \quad (64)$$

$$Q_{s\pm} = (\xi_{s\pm} - a)^2. \quad (65)$$

These equations are equivalents to (2.12) and (2.13) of [13].

Each of  $z_{s\pm}$  solutions has a maximum in the interval  $1 \leq z \leq \infty$ , that corresponds with  $z_{\pm M} = z_{a,b}$ ,  $x_{\pm M} = x_{ea,b}$  defined in (63). Beyond these points they decay asymptotically to one, as we can see in figure (5).

As you can see in the last figure, if

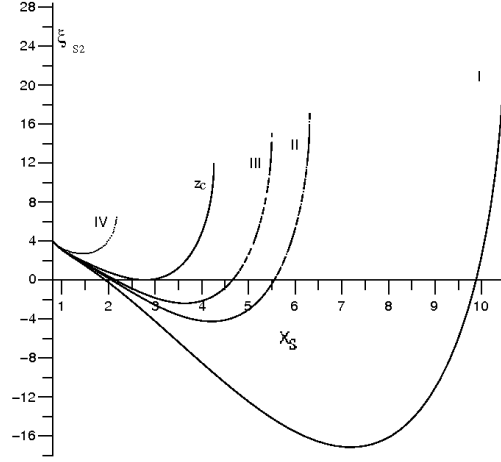
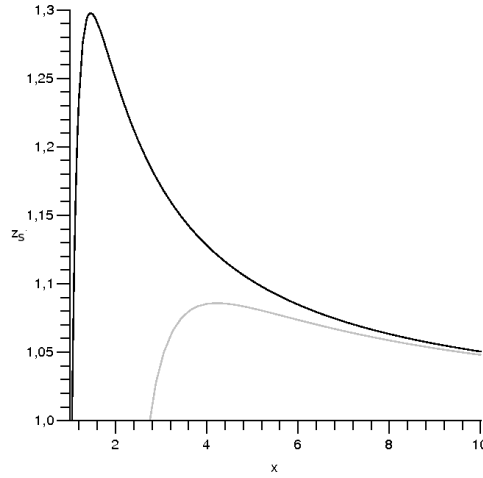


Figure 4:

Figure 5: Graphic  $z(x_s)$ ,  $\eta = 0$ ,  $a = 0.8$ 

- $1 < z < z_b$  we have four spherical orbits.
- $z = z_b$  we have three, one of them in  $x_{eb}$  such that  $\{z_b, x_{eb}, a\}$  are solutions of (62),(63) equations ( $z_b < z_a$ ),
- $z_b < z < z_a$  we have two,
- $z = z_a$  we have the last one, such that  $\{z_a, x_{ea}, a\}$  are its solutions.

A specially simple expression of the function  $z_{s\pm}(x_s, a)$  can be obtained for  $z = 1$ , and  $z = 9/8$  values, that are well known in the literature.

$$a(z=1) = \sqrt{4(x_s - 2\sqrt{2x_s} + 2)x_s} = 2\sqrt{x_s(\sqrt{x_s} - \sqrt{2})^2}. \quad (66)$$

$$a(z=9/8) = \frac{2\sqrt{2x_s}}{9} \sqrt{-7x_s^2 + 18x_s + 81 \pm 4(9 - x_s)\sqrt{x(9 - 2x_s)}}. \quad (67)$$

(See [13] and [7] for details).

**F** *Schwarzschild circular orbits.*

Conditions  $R = R' = 0$  imply

$$\xi_{s\pm} = \pm \frac{\sqrt{2x_s^{\frac{3}{2}}}}{x_s - 1} \quad (68)$$

$$z_s = \frac{(2x_s - 3)x_s}{2(x_s - 1)^2}. \quad (69)$$

$$\mathcal{Q}_{s\pm} = \xi_{s\pm}^2. \quad (70)$$

Functions  $\xi_{s-}$  and  $z_s$  have a maximum,  $\xi_{s-M} = -\frac{3\sqrt{6}}{2}$ ,  $z_{sM} = 9/8$  respectively, in  $x_s = 3$ , and  $\xi_{s+}$  a minimum,  $\xi_{s+m} = \frac{3\sqrt{6}}{2}$ .

Stable circular orbits can be found when  $3 < x_s < \infty$ , and unstable  $2 \leq x < 3$ , where  $x_s = 2, z_s = 1, \xi_{s\pm} = \pm 4$  corresponds to the inner unstable circular orbit. (See [13] and [7] for details).

## 5 Spherical orbits in the $\hat{Q} - \hat{L} - \hat{E}$ space

In this section we are interested in representing “outer” spherical orbits in a  $\hat{Q}$ ,  $\hat{L}$  and  $\hat{E}$  (1) formal three-space, ( $\hat{Q} = z^{-1}\mathcal{Q}$ ,  $\hat{L} \equiv z^{-1/2}\xi$  and  $\hat{E} \equiv z^{-1/2}$ ), analyzing their properties, as we have mentioned before. This task can be achieved due to the special shape of the geodesic equation that, at the same time, derives from the existence of two killing vector fields and one conformal killing 2-tensor. As we have seen  $\xi_{s2}$  and  $\mathcal{Q}_{s2}$  depend exclusively on  $x = r/2m$  coordinate. This fact allow us to construct a formal three space in such a way that the whole set of spherical orbits will be represented by a 2-surface, say  $\Sigma$ , in this space. In the next chapter we will see that orbits with non null eccentricity can be represented in the same formal space. Therefore, we will achieve a global and careful (with accurate analytical control) representation of the whole set of orbits in Kerr space-time.

**A.** Each point of this space is characterized by their coordinates  $\mathcal{X}^i \equiv \{\hat{Q}, \hat{L}, \hat{E}\}$ .

The geometrical locus of the spherical orbits in this space is a 2-surface  $\Sigma$  defined by:

$$\begin{aligned} \hat{Q} &= z^{-1}\mathcal{Q}_{s2}(x_s, z, a), \\ \hat{L} &= z^{-\frac{1}{2}}\xi_{s2}(x_s, z, a), \\ \hat{E} &= z^{-\frac{1}{2}}, \end{aligned} \quad (71)$$

limited by

$$\hat{Q} = (\hat{L} - a\hat{E})^2, \quad (72)$$

that is, the surface representing the equatorial plane in this space ( $\eta = 0$ ), and  $0 < \hat{E} \leq 1$ . Finally  $x_s$  and  $z$  ( $z = \hat{E}^{-2}$ ) have to be considered the two parameters constrained by

$$\begin{aligned} x_+(a) &\leq x_s \leq x_{s_{max}}(z), \\ 1 &< z \leq z_a(a). \end{aligned}$$

where  $z_a$  is defined in (62). We will look at this representation  $a$  ( $0 < a \leq 1$ ) as a constant (for example  $a = 0.8$ ), discussing its variation in the results and including  $z = 1$  as a limiting case.

Moreover, this representation is not sensitive to initial conditions. Then, one point represents spherical orbits but, in some circumstances, the same point represents the associated geodesics (see next section for definition).

It is well known (see [14] for example) that singular points occur when two minors of the matrix

$$\begin{pmatrix} \frac{\partial \hat{Q}}{\partial x_s} & \frac{\partial \hat{L}}{\partial x_s} & \frac{\partial \hat{E}}{\partial x_s} \\ \frac{\partial \hat{Q}}{\partial z} & \frac{\partial \hat{L}}{\partial z} & \frac{\partial \hat{E}}{\partial z} \end{pmatrix} = 0 \quad (73)$$

vanishes. This condition holds if and only if  $\xi'_{s2} = \mathcal{Q}'_{s2} = 0$ . The solution of these equations is  $x_s = x_e(z, a)$ . Replacing this solution in (71) we obtain the set of singular points of  $\Sigma$ .

### B.

Spherical orbits can be represented using a parametric plot of equations (71). The range of variation of parameters  $x_s$  and  $z$  are such that the surface  $\Sigma$  is limited by  $\hat{E} = 1$  plane and the surface  $\hat{Q} = (\hat{L} - a\hat{E})^2$  as is shown above. In figure (6) we depict the intersections of these surfaces, including slices obtained cutting  $\Sigma$  by planes of  $z = \text{constant}$ , as we explain below, for a particular values of  $a$ .

In this figure we can see how  $\Sigma$  is in fact a surface folded by the line from point  $A$  to point  $C_3$  made of singular points. The equation of this line has been found in (49), (50) and (51). Each point represents the spherical orbit with the maximum value of  $\hat{Q}$  and the minimum of  $\hat{L}$  for a fixed value of  $z$  and  $a$ .

Unstable spherical orbits are represented by the points of the lower pseudo-trapezoid face with curved sides (that we represent by a widehat over the extrema of the piece of curve). These sides are:

- $\widehat{A, E_1}$  and  $\widehat{C_3, E_{32}}$ , unstable circular orbits on the equatorial plane,
- $\widehat{A, C_3}$ , singular points of  $\Sigma$ ,
- $\widehat{E_1, E_{32}}$ , unstable spherical orbits with  $\hat{E} = 1$ .

Stable spherical orbits form a partially unlimited face with sides:

- $\widehat{A, C_3}$ , singular points of  $\Sigma$ ,
- $\widehat{A, E_2}$  and  $\widehat{C_3, E_{31}}$ , stable circular orbits on the equatorial plane.

The apexes of these partially non-limited volume are:

- $A$  the circular orbit in the equatorial plane with smallest value of  $\hat{E}$  for a fixed value of  $a$ .

- $E_1$  and  $E_{32}$  circular unstable orbits in the equatorial plane with  $\hat{E} = 1$ ,
- $C_3$  circular orbit in the equatorial plane with smallest value of  $\hat{E}$  and  $\hat{L} < 0$ .
- $E_2$  and  $E_{31}$  limiting points representing stable circular orbits in the equatorial plane when  $\hat{E} \rightarrow 1$

We complement our knowledge of  $\Sigma$  cutting slices of  $\hat{E} = \text{constant} (\Leftrightarrow z = \text{constant})$ . Then, the spherical orbits could be represented in each slice in a parametric way by (71) where  $z$  takes a constant value. We include the intersection of each slice with the surface of the equatorial plane.

The complexity of the behavior of these parametric functions forces the study of their particular shape for the cases studied in table 1. Relations listed in the previous chapter allow us to better understand those particular shapes.

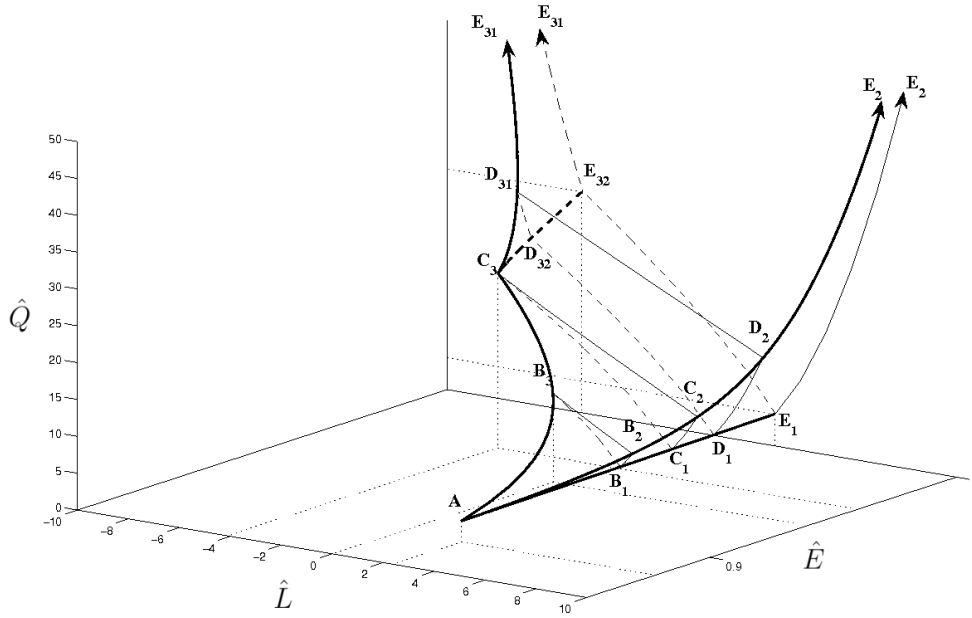


Figure 6: The geometrical locus of spherical orbits in Kerr space time. Slices are made for  $I, z = 1.05$ ;  $II, z = z_b = 1.086$ ;  $III, z = z_c = 1.133$ ;  $IV, z = z_a = 1.298$

- **Case 0:**  $z = 1$ .  $\widehat{E_1, E_{32}}$  unstable spherical orbits with  $\hat{E} = 1$
- **Case I:**  $1 < z < z_b$ .  $\widehat{D_1, D_{32}}$  unstable spherical orbits,  $\widehat{D_2, D_{31}}$  stable spherical orbits,
- **Case II:**  $z = z_b$ .  $\widehat{C_1, C_3}$  unstable spherical orbits,  $\widehat{C_2, C_3}$  stable spherical orbits  $\hat{E} = z_b^{-1/2}$ ,
- **Case III:**  $z_b < z = z_c < z_a$   $\widehat{B_1, B_3}$  unstable spherical orbits,  $\widehat{B_2, B_3}$  stable spherical orbits  $\hat{E} = z_c^{-1/2}$ ,



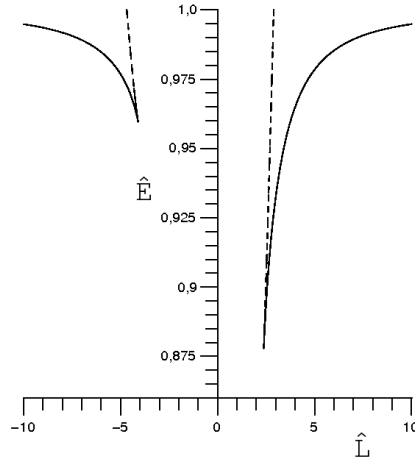


Figure 7:  $\hat{L} - \hat{E}$  plot of circular orbits on the equatorial plane,  $\hat{Q} = (\hat{L} - a)^2$ .

- **Case IV** :  $z = z_a$  Last stable spherical orbit.

In order to complement the previous plots, we add the projection on the  $\hat{E}, \hat{L}$  plane of the spherical orbits on the equatorial plane. We represent these orbits on a parametric plot using (64) into (71). See figure (7) plotted for  $a = 0.8$ , that are the projections of  $\widehat{A}, \widehat{E}_1$ ,  $\widehat{A}, \widehat{E}_2$ ,  $\widehat{C}_3, \widehat{E}_{31}$  and  $\widehat{C}_3, \widehat{E}_{32}$ .

As  $a$  decreases both peaks of this  $\hat{L} - \hat{E}$  plot become more and more symmetric until we arrive to  $a = 0$ , where they become completely symmetric (as could be expected from the spherical symmetry of Schwarzschild black holes)

**C** As we have seen in section D of the previous chapter, in the general case I, the function  $\mathcal{Q}_{s2}$  has four values of  $x_s$ , say  $x_i$   $i \in \{1, 2, 3, 4\}$ , such that  $\mathcal{Q}_{s2} = (a - \xi_{s2})^2$ , for a fixed value of  $a$  and  $z$ . The plots have been obtained in all cases increasing the value of the  $x_s$  parameter, first from  $x_1$  to  $x_2$  (in figure 6 from  $D_1$  to  $D_{32}$ ) for the unstable branch, and from  $x_3$  to  $x_4$  for the stable one (from  $D_{31}$  to  $D_2$ ). In the other cases the end of the unstable and the start of the stable branches is  $x_e$  which traces the singular points of the global surface.

We can now show the relative values of  $\xi_{s2}(x_i, z, a)$ , that is

	$x_i$	$\xi_{s2}(x_i, z, a) \equiv \xi_i$
<i>I</i>	$x_1 < x_2 < x_3 < x_4$	$\xi_3 < \xi_2 < 0 < \xi_1 < \xi_4$
<i>II</i>	$x_1 < x_2 = x_3 < x_4$	$\xi_3 = \xi_2 < 0 < \xi_1 < \xi_4$
<i>III</i>	$x_1 < x_4$	$0 < \xi_1 < \xi_4$
<i>IV</i>	$x_1 = x_4$	$0 < \xi_1 = \xi_4$

Moreover, since  $\xi_{s2}$  is a continuous function, it has a minimum in  $x_e$  and takes positive values in the extrema of  $\mathcal{D}$ ,  $x_+$  and  $x_{smax}$ , from the above table, we can infer that  $\xi_{s2} = 0$  in two

points  $x_l$  ( $\xi'_{s2}(x_l, z, a) < 0$ ) and  $x_m$  ( $\xi'_{s2}(x_m, z, a) > 0$  and  $x_l < x_m$ ) if  $1 < z \leq z_c$ . Thus: i)  $x_1 < x_l < x_2 < x_3 < x_m < x_4$  in the case I and II, ii) if  $z_b < z < z_c$ , then  $x_e < x_l < x_1$  and  $x_e < x_m < x_4$ , iii) if  $z = z_c$  then  $x_e = x_l = x_m$ .

**D** *Continuously moving in a geometrical locus of spherical orbits.* Let us choose  $P$ , a point of  $\Sigma$ . The holonomic base of the tangent space in  $P$  associated to curves on  $\Sigma$  of  $x_s = \text{constant}$  and  $z = \text{constant}$  is

$$\mathbf{X}_z \equiv \frac{\partial}{\partial z} = \hat{Q}_z \frac{\partial}{\partial \hat{Q}} + \hat{L}_z \frac{\partial}{\partial \hat{L}} + \hat{E}_z \frac{\partial}{\partial \hat{E}} \quad (74)$$

$$\mathbf{X}_{x_s} \equiv \frac{\partial}{\partial x_s} = \hat{Q}' \frac{\partial}{\partial \hat{Q}} + \hat{L}' \frac{\partial}{\partial \hat{L}}, \quad (75)$$

where  $\hat{Q}'$  and  $\hat{Q}_z$  means partial differentiation of  $\hat{Q}_{s2}$  with respect  $x_s$  and  $z$  respectively and  $\frac{\partial}{\partial \hat{Q}}, \frac{\partial}{\partial \hat{L}}, \frac{\partial}{\partial \hat{E}}$  is the holonomic base on  $P$  of  $\hat{Q}, \hat{L}, \hat{E}$  space.

As a consequence of gravitational radiation, in the adiabatic approximation, a test particle can follow a trajectory that can be imagined as a chain of orbits in such a way that the particle remains several periods on each orbit before changing to another orbit. We define  $\mathbf{t}$  as an average over several orbital periods. According to this, the constants of motion ( $\hat{Q}, \hat{L}, \hat{E}$ ) associated to different orbits vary according to a law that evolves  $d\hat{Q}/dt, d\hat{L}/dt, d\hat{E}/dt$  quantities. In fact, the solution of the first order ordinary equations is a curve in our formal space such that

$$\mathbf{V} = \frac{d\hat{Q}}{dt} \frac{\partial}{\partial \hat{Q}} + \frac{d\hat{L}}{dt} \frac{\partial}{\partial \hat{L}} + \frac{d\hat{E}}{dt} \frac{\partial}{\partial \hat{E}}, \quad (76)$$

where  $\mathbf{V} \equiv d/dt$ , is its tangent vector ( $\cdot \equiv d/dt$ ). The necessary and sufficient condition to ensure us that a particle in spherical motion remains in a spherical orbit under the influence of radiation reaction is

$$\epsilon_{ijk} V^i X_{x_s}^j X_z^k = 0 \Leftrightarrow \quad (77)$$

$$\hat{L}' \frac{d\hat{Q}}{dt} = \frac{\hat{Q}_z \hat{L}' - \hat{Q}' \hat{L}_z}{\hat{E}_z} \frac{d\hat{E}}{dt} + \hat{Q}' \frac{d\hat{L}}{dt}, \quad (78)$$

where  $\epsilon_{ijk}$  is the Levi-Civita tensor. Hence, equation (78) becomes [12], (see also equation 3.25 of [3])

$$\frac{d\hat{Q}}{dt} = 2 \frac{2x_s + \sqrt{-2x_s(-z - 2x_s + 2zx_s)}}{(2x_s - 1)\sqrt{z}} [(a^2 + 4x_s^2) \frac{d\hat{E}}{dt} - a \frac{d\hat{L}}{dt}]. \quad (79)$$

If the motion lies entirely on the equatorial plane then equation (78), taking into account (72), becomes

$$\frac{d\hat{E}}{dt} \hat{L}_z = \frac{d\hat{L}}{dt} \hat{E}_z. \quad (80)$$

The result is

$$\frac{d\hat{L}}{dt} = -\frac{d\hat{E}}{dt} \frac{1}{(2x - 1)a} (4x^2 + a^2 + \frac{2^{3/2}x^2\Delta}{\sqrt{-x(2zx - 2x - z)}}). \quad (81)$$

Using basic instruments of classical differential geometry we can find the necessary and sufficient condition for a stable spherical geodesic be able to achieve a non null eccentricity orbit following  $\mathbf{V}$  direction, that is,  $\epsilon_{ijk} V^i X_{x_s}^j X_z^k < 0$ . This result applies if the start point is an unstable

spherical orbit and we want to achieve a non null eccentricity orbit in  $\mathbf{V}$  direction. In general this construction allow us if whether or not a specific curve, with  $\mathbf{V}$  as a tangent vector in each point, is inside this partially unlimited volume of orbits in Kerr space time, and therefore if this is able to describe the path of a radiating particle in the adiabatical approximation.

## 6 Non-null eccentricity Orbits in the $\hat{Q} - \hat{L} - \hat{E}$ space

In the previous section we have constructed a space where we have placed the spherical orbits, now we are going to study all orbits and we will see that spherical ones delimitate where the rest of the orbits are.

**A The  $U$  potential.** In order to analyze the non null eccentricity orbits in relation to the spherical ones we could use the potential technique factorizing  $R$  as follows,

$$R = T(\hat{U} - \hat{Q}), \quad (82)$$

where  $T$  and  $\hat{U}$  are defined below. The complexity of  $\hat{U}$  advise us to use  $\eta$  to factorize  $R$ . It will be easy to translate the results in terms of  $\hat{Q}$  and  $\hat{L}$  as we show below.

According to (39) we have

$$R = \frac{\Delta}{4}[U - \eta], \quad (83)$$

$$\begin{aligned} U &= \frac{4x^2}{x-1}[z - (z-1)x] - \frac{4x(x-1)}{\Delta}(\xi + \frac{a}{x-1})^2 = \\ &= -\frac{4x\{4(z-1)x^3 - 4zx^2 + [\xi^2 + (z-1)a^2]x - (\xi-a)^2\}}{4x^2 - 4x + a^2}. \end{aligned} \quad (84)$$

Therefore, considering that  $T(\hat{U} - \hat{Q}) = \frac{\Delta}{4}(U - \eta)$ , we obtain

$$\hat{U} = zU - z(\xi - a)^2, \quad (85)$$

$$T = \frac{\Delta}{4z},$$

$$\hat{Q} = z^{-1}[\eta + (\xi - a)^2]. \quad (86)$$

Orbits exist only if  $R \geq 0$ . This implies

$$U \geq \eta. \quad (87)$$

For fixed values of  $\xi$  and  $z$  parameters, and  $a$ ,  $U$  depends on  $x$ .

- $x \rightarrow x_+$  then  $U \rightarrow +\infty$
- $x \rightarrow \infty$  then  $U \rightarrow -\infty$
- $U$  is continuous in the domain:  $0 < a \leq 1$ ,  $1 < z$ ,  $x_+ < x < \infty$
- Using Descartes's rule on the third-degree polynomial part (see(84)), one can see that, for the values of  $a$ ,  $z$  and  $\xi$  that we are interested in, there are always 3 changes of sign. Thus there's the possibility of having at most 3 real roots, and we know that there will be at least 1 root, because this function, being continuous, goes from  $\infty$  to  $-\infty$  inside that region.

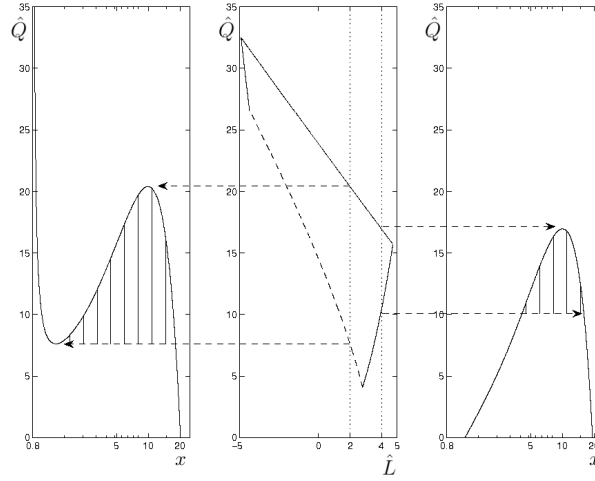


Figure 8: Relationship between  $\hat{Q} - \hat{L}$  plot and  $\hat{U}$  potential in two scenarios: at left  $\hat{L}_0 = 2$  intersects the stable and unstable curves and so we have both extrema of  $\hat{U}$  above the minimum value of  $\hat{Q}$ , i.e 1.48 ( $\Leftrightarrow \eta = 0$ ). At right  $\hat{L}_0 = 4$  only intersects the stable orbits curve and then we only have the maximum of  $\hat{Q}$  above the minimum allowed value of  $\hat{Q}$ , 10.36. Regions where orbits exist are filled with vertical lines.

Extrema of  $U$  can't be found analytically. As it has been explained, the conditions for spherical orbits are  $R = 0$  and  $R' = 0$ . In  $U$  potential terms, they are equivalent to:

$$\eta = U(x, a, \xi, z) \quad (88)$$

$$U'(x, a, \xi, z) = 0 \quad (89)$$

The set of values of  $\xi, \eta, z, x, a$  which correspond to spherical orbits are related through the functions  $\xi_{s1,2}$  and  $\eta_{s1,2}$ . We are going to study the extrema of  $U$  through these functions proceeding as follows: First, one value of  $a_0$  and  $z_0$  is chosen. Then, to completely define the  $U$  potential, we have to choose a particular value of  $\xi$ , say  $\xi_0$ .

The two functions  $\xi_{s1,2}$  coincide at the extrema of the interval of  $x_+ \leq x \leq x_{smax}$ . They are continuous functions and each one has one extremum in the interval, a minimum for  $\xi_{s2}$  and a maximum for  $\xi_{s1}$ . So they form a oval closed shape. Hence, we can find different scenarios depending on  $\xi_0$ :

- $\xi_0$  is such that  $\xi_0 > \xi_{s1}$  or  $\xi_0 < \xi_{s2}$ . Thus  $U$  doesn't have any extremum.
- $\xi_0$  is tangent to the oval shape at  $\xi_{s1}$  maximum or  $\xi_{s2}$  minimum. In this case  $U$  potential has an inflection point.
- $\xi_0$  intersects twice the shape. This implies that two extrema exist in D. In this case, intersections with  $\xi_{s1}$  curves implies that the corresponding extrema are below the horizontal

axis since  $\eta_{s1} < 0$ . But for intersections with  $\xi_{s2}$  the extremum will be over or below the horizontal axis depending on the sign of  $\eta_{s2}$ .

As we have seen,  $U$  is a continuous function that takes the values  $+\infty$  and  $-\infty$ , at  $x_+$  and  $x \rightarrow \infty$ , respectively. Then if it has two extrema, it must first have a minimum, and after a maximum, with the maximum being above the minimum.

In figure (8) we can see the more general example where the two possible scenarios are plotted in terms of  $\hat{Q}$  and  $\hat{L}$  by using (85), and (86) (the form of  $\hat{U}$  is like  $U$  except a shift and a rescaling). We have complemented the information comparing these two plots with the corresponding  $\hat{Q}$  versus  $\hat{L}$ , that corresponds to the Case I (slice  $D_1, D_2, D_{31}, D_{32}$  of figure (6) of the previous section), establishing graphical analogies.

Now that we know the shape of  $\hat{U}$  we can find where the non-spherical orbits are. An orbit must exist between two turning points, if we choose a value  $\hat{Q}_0$  we see that it can intersect up to three times the  $\hat{U}$  potential defining three turning points  $x_t \leq x_a \leq x_p$ . We can find orbits only when  $\hat{Q}_0$  value is between both  $\hat{U}$  extrema (considering  $\hat{Q}_0 \geq (\hat{L}_0 - a\hat{E}_0)^2$ , where  $\hat{L}_0$  and  $\hat{E}_0$  are fixed values defining  $\hat{U}$ ) and  $x_a \leq x \leq x_p$ , such that the apoaster is in  $x_a$ , and the periaster is in  $x_p$ . This situation corresponds to the region between the two curves at the  $\hat{Q}$  versus  $\hat{L}$  plots and the curves  $\eta = 0 \Leftrightarrow \hat{Q} = (\hat{L} - a\hat{E})^2$ . Geodesics falling into the hole exist in  $x_+ \leq x \leq x_t$  region (associated geodesics [7]), assuming the same values of the physical parameters  $\hat{Q}_0$ ,  $\hat{L}_0$  and  $\hat{E}_0$  of the associated orbits.

Figure (8) tell us that, starting from a value of  $\hat{Q}_0$  corresponding to an orbit, if we increase continuously this value we can achieve at most the value  $\hat{U}_{max}$  in order to have physical orbits. But if we decrease this value in the left case of (8) below  $\hat{U}_{min}$  we will get open geodesics that will be swallowed by the hole, but at the right case of (8), if  $\hat{Q}_0 < (\hat{L} - a\hat{E})^2$  no physical orbits exist. Therefore, the surfaces representing stable spherical orbits and the  $\hat{Q}_0 = (\hat{L} - a\hat{E})^2$  surface in figure (6) are impenetrable, i.e. can be achieved but not crossed following a continuous change of the physical parameters from an interior point of the volume of orbits, while the surface of unstable spherical orbits can bidirectionally be crossed.

### B The region where orbits exist.

If we focus on  $1 < x$  region we can obtain interesting results due to the fact that, in that region,

$$0 \leq \eta \leq U(\xi, z, x, a) \leq h(x, z) \quad (90)$$

since

$$U = h - \frac{4x(x-1)}{\Delta} \left( \xi + \frac{a}{x-1} \right)^2 \quad (91)$$

$$h = \frac{4x^2}{x-1} [z - (z-1)x]. \quad (92)$$

If  $x \rightarrow 1+$  then  $h \rightarrow +\infty$ , if  $x \rightarrow +\infty$  then  $h \rightarrow -\infty$ , besides if  $1 < z \leq 9/8$  has a minimum in  $x_{e1}$  and a maximum in  $x_{e2}$ ,  $x_{e1} \leq x_{e2}$  and  $h(x_{e1}, z) \leq h(x_{e2}, z) > 0$ , and if  $9/8 < z$ , thus  $h(x, z)$  is a continuously decreasing function. In addition to this  $h(x, z) \geq 0 \Leftrightarrow 1 < x \leq x_{limit}$ , where

$$x_{limit} \equiv z/(z-1). \quad (93)$$

Considering that  $h(x, z) < 0$  in the  $x_+ \leq x \leq 1$  region, we can assert that the allowed values of  $x$  coordinate of orbits are bounded by  $x_+ < x \leq x_{limit}(z)$ . The upper limit only depends on mass energy ratio.

**C Orbits co rotating with the hole**

According to figure 6, physical orbits with  $z \geq z_c$  are characterized by  $\hat{L} \geq 0$  ( $\Leftrightarrow \xi \geq 0$ ). In fact, there exists a set of orbits with the same value of  $\hat{L}$ . These orbits are placed in this figure in the slice of  $\hat{L} = \text{constant} \geq 0$ , including a number of stable and unstable orbits. Therefore Theorem IV must be extended beyond spherical orbits, concluding that all orbits with  $z \geq z_c$  co rotate with the hole. That is, following (14) we can check that  $d\phi/d\tau \geq 0$  for all orbits with  $z \geq z_c$ .

$$\frac{z^{\frac{1}{2}} \bar{\rho}^2}{2} \frac{d\phi}{d\bar{\tau}} = \left( \frac{1}{1-\mu^2} - \frac{a^2}{\Delta} \right) \xi + \frac{4ax}{\Delta} \geq \left( 1 - \frac{a^2}{\Delta} \right) \xi + \frac{4ax}{\Delta}. \quad (94)$$

But, we can always find a spherical orbit such that  $\xi = \xi_{s2}$ . Thus

$$\left( 1 - \frac{a^2}{\Delta} \right) \xi + \frac{4ax}{\Delta} - \xi = \left( 1 - \frac{a^2}{\Delta} \right) \xi_{s2} + \frac{4ax}{\Delta} - \xi_{s2} = \frac{a \left( 1 + \sqrt{2} \sqrt{-(-2x + 2zx - z)x} \right)}{2x - 1} > 0. \quad (95)$$

Therefore

$$\frac{z^{\frac{1}{2}} \bar{\rho}^2}{2} \frac{d\phi}{d\bar{\tau}} = \left( \frac{1}{1-\mu^2} - \frac{a^2}{\Delta} \right) \xi + \frac{4ax}{\Delta} > \xi. \quad (96)$$

## 7 Summary of main results

The main goal of this paper has been to provide different tools in order to have a very important knowledge of both (unstable and stable) spherical orbits, and non null eccentricity orbits in the outer Kerr space time, studying how their physical parameters are related. This is due to the special role played by Kerr orbits to explain astrophysical effects in strong gravitational fields such as gravitational wave radiation in the adiabatic approximation.

To achieve this, we have developed an analytical study of orbits out of the equatorial plane, recovering, as expected, classical results of orbits lying entirely on the plane of symmetry including the Schwarzschild results and the limit of Kerr metric ( $a = 1$ ). A numerical approach to obtain specific results about orbits or radiative models can be implemented based on our analytical approach.

1) We have classified spherical orbits in 4 different classes according to the different behavior of the physical parameters restricted to spherical orbits  $\hat{Q}_{s2}$ ,  $\hat{L}_{s2}$  and  $\hat{E}$ . The influence of  $a$  in the results has been studied, as well as maximum values, domain of existence and correlations of  $\hat{Q}_{s2}$  with  $\hat{L}_{s2}$ , showing that these two functions have a common extremum in  $e$  ( a minimum of  $\hat{L}_{s2}$  and a maximum of  $\hat{Q}_{s2}$ ) that, at the same time, is the threshold that divides stable and unstable spherical orbits (see Theorem II).

2) Moreover, using the properties of the extremum  $e$  mentioned above, we have found that, for  $z > z_c(a)$  ( $\Leftrightarrow \hat{L}_{s2} \geq 0$ ), all orbits (including the spherical ones) have a positive value of  $\hat{L}$  and therefore must co-rotate with the hole.

3) According to this classification we have constructed the physical parameters space  $(\hat{Q}, \hat{L}, \hat{E})$  showing that the whole set of spherical and non-null eccentricity orbits can be represented there.

We have been able to carry this out thanks to the fact that the Kerr metric has two killing vectors and one killing 2-tensor and the choice of Boyer-Linquist coordinates. In this space the geometrical locus of spherical orbits is a 2-surface that looks like two sheets (one for stable and the other for unstable spherical orbits), partially matched through a common curve. We have proved that this curve is the set of singular points of this 2-surface characterized by the condition  $\hat{Q}'_{s2} = \hat{L}'_{s2} = R'' = 0 \Leftrightarrow x_s = x_e(z, a)$ .

This surface can be constructed using slices of  $z = \text{constant}$ . Each slice exhibits the limits of  $\hat{Q}$  and  $\hat{L}$  values, showing that beyond  $z_a(a)$  no physical orbits ( $\eta \geq 0$ ) exist. It means that if  $E < E_a = m\sqrt{z_a}$  neither spherical nor non null eccentricity orbits exist. The larger value of  $z_a$  is 3 for  $a = 1$ .

4) Studying the  $U$  potential we have seen that non-null eccentricity orbits are placed in this formal three-space between the two sheets of stable and unstable spherical orbits and limited by the surface representing the equatorial plane. Then, we obtained a global representation of the whole set of orbits in the outer region of the Kerr space-time. This representation allows us to see whether or not a particle can achieve one specific orbit from another one with a continuous change of its parameter values.

5) Using a property of  $U$  potential, we have obtained  $x_{limit}$  (see (93)), that is, a maximum value for the  $x$  coordinate of an orbit (spherical or not) depending on its energy-mass relation,  $\hat{E}$ .

6) We have obtained the necessary and sufficient condition that the variations of the  $\hat{Q}$ ,  $\hat{L}$  and  $\hat{E}$  parameters must hold so that a spherical orbit remains spherical. Using this condition, we recover the result obtained in [10] in the Schwarzschild limit and small perturbations of a stable spherical orbit, and in [12] in Kerr space-time.

7) Variations of the parameters due to gravitational radiation in the adiabatical approximation can be represented in this formal space as a curve going from one geodesic to another. Therefore we can check whether or not this path is possible according to the fact that the upper sheet of  $\Sigma$  (that of stable spherical orbits) is impenetrable while the lower one is not, as has been proved in section 6. This representation, as a formalization of analytical results, can be an important tool to check whether a transition from one orbit to another is valid or not.

In particular the necessary condition to go from one stable spherical geodesic to an unstable one (or vice versa) following a way that only include spherical orbits is crossing the singular line of  $\Sigma$ .

## 8 Appendix I

In order to prove that  $\eta_{s1} < 0$  in  $\mathcal{D}$ , we can do the next changes of variable and parameter: a)  $z = 2x_{smax}/(2x_{smax} - 1)$ , b)  $x_s = t_s + x_+$  and c)  $x_{smax} = t_{smax} + x_+$  (then  $0 \leq t \leq t_{smax}$ ) where  $x_{smax}$  is defined in (33) and  $x_+$  is the outer horizon. After applying this changes, we obtain

$$\eta_{s1} = -\frac{4x_s^2}{(2x_s - 1)^2 a^2} [J(x_s, a, z) + 2\Delta \sqrt{2x_s(2(1-z)x_s + z)}], \quad (97)$$

where

$$J(x_s, a, z) \equiv j(t_s, a, t_{smax}) =$$

$$\begin{aligned}
& + \frac{8}{2t_{smax} + \sqrt{1-a^2}}[2(t_{smax} - t_s) + 4]t_s^3 + \\
& + 4[6\sqrt{1-a^2}(t_s - t_{smax}) + (3(\sqrt{1-a^2} - 2))]t_s^2 \\
& + 4[(1-a^2) + 4(1-a^2)t_{smax} + \sqrt{1-a^2}]t_s + \\
& + (1-a^2)[4t_{smax} + 4t_{smax}\sqrt{1-a^2} + 2\sqrt{1-a^2} + (2-a^2)]
\end{aligned} \tag{98}$$

This implies that  $\eta_{s1} < 0$  in the intervals of interest, q.e.d..

## 9 Appendix II

After some manipulations we can see that the system of equations  $\xi'_{s2} = \mathcal{Q}'_{s2} = 0$  is equivalent to

$$0 = a^2 + G(x_s, z), \tag{99}$$

where

$$\begin{aligned}
G(x_s, z) &= -\frac{4x_s}{z^2}\{8(z-1)(z-2)x_s^2 + 3z(4-3z)x_s + 3z^2 + \\
&+ 4[2(z-1)x_s - z]\sqrt{2x_s[2(1-z)x_s + z]}\}.
\end{aligned} \tag{100}$$

In fact, functions  $\xi'_{s2}$  and  $\mathcal{Q}'_{s2}$  can be written

$$\xi'_{s2}(x_s, a, z) = \frac{H(x_s, z)}{a}[a^2 + G(x_s, z)], \tag{101}$$

$$\mathcal{Q}'_{s2}(x_s, a, z) = \frac{F(x_s, z)}{a^2}[a^2 + G(x_s, z)], \tag{102}$$

where  $F(x_s, z) \neq 0$  and  $H(x_s, z) \neq 0$ .

We define functions  $S(x, a, z)$  according to

$$S(x, a, z) = G(x, z) + a^2 = \tag{103}$$

$$\begin{aligned}
&= a^2 - \frac{4x}{z^2}[8(z-1)(z-2)x^2 + 3z(4-3z)x + 3z^2] - \\
&- \frac{16x}{z^2}[2(z-1)x - z]\sqrt{-2x[2(z-1)x - z]}.
\end{aligned} \tag{104}$$

We implement the change of variable

$$x \rightarrow y = \frac{x}{x_{smax}} - 1/2, \tag{105}$$

where  $x_{smax}$  has been defined in (33).

This change implies that  $x = 0 \leftrightarrow y = -1/2$  and  $x = x_{smax} \leftrightarrow y = +1/2$ . At the same time  $y = 0 \leftrightarrow x = x_{smax}/2$ . In addition to this

$$x_+ \leftrightarrow y_+ = \frac{1}{2} - \frac{1}{z} + (1 - \frac{1}{z})\sqrt{1-a^2}. \tag{106}$$

Now, the position of the outer horizon  $y_+$  depends not only on  $a$  but also on  $z$ . Remember that the domain  $\mathcal{D}$  exists iff. condition  $x_+ \leq x_{smax}$ ,  $\Leftrightarrow 1 - (z-1)\sqrt{1-a^2} \geq 0$  holds.



The dependence of function  $S$  on  $y$  is

$$S(y, z, a) = a^2 - \frac{z}{(z-1)^2} [4(z-2)y^3 - 3zy^2 + \frac{5}{4}z - 1] + \quad (107)$$

$$+ \frac{z}{(z-1)^{3/2}} (1 - 4y^2)^{3/2}. \quad (108)$$

The values of  $S$  in the following points are

$$S(y = -\frac{1}{2}) = a^2 \geq 0, \quad (109)$$

$$S(y = +\frac{1}{2}) = a^2 - 1 + \frac{1}{(z-1)^2} = \frac{(1 - (z-1)\sqrt{1-a^2})^2}{2(z-1)\sqrt{1-a^2}} \geq 0, \quad (110)$$

$$S(y = 0) = -a^2 + \frac{z[5(z-1) - 4(z-1)^{1/2} + 1]}{4(z-1)^2} < 0, \quad (111)$$

$$\begin{aligned} S(y_+) &= -\frac{4}{z^2} \{ (1 - (z-1)\sqrt{1-a^2})(1 + \sqrt{1-a^2}) \times \\ &\times [\sqrt{1 - (z-1)\sqrt{1-a^2}} - \sqrt{1-a^2}]^2 \} < 0. \end{aligned} \quad (112)$$

As a direct consequence we see that  $S(\pm 1/2) \geq 0$ ,  $S(0)$  is a negative function of  $z$ , ( $1 < z$ ), such that  $S(0) < a^2 - 1$ , and  $S(y_+) \geq 0$ .

Moreover,

$$S'(y) = \frac{6zy}{(z-1)^2} [2(z-2)y - z + 2(z-1)^{1/2}(1-4y^2)^{1/2}]. \quad (113)$$

The equation  $S'(y) = 0$  has two solutions in

$$\begin{aligned} y_1 &= 0, \\ y_2 &= \frac{1}{2} - \frac{1}{z}, \quad S(y_2) = a^2 - 1. \end{aligned} \quad (114)$$

It is crucial to see that

$$y_+ = y_2 + (1 - \frac{1}{z})(1 - a^2)^{1/2} \Rightarrow y_+ \geq y_2, \quad (115)$$

and  $S(0) = S(y_1) < S(y_2) \leq 0$ .

Considering these previous results, and taking into account the continuity of  $S$ , we can assert that this curve has at least one root ( $S = 0$ ) in the interval  $-1/2 < y \leq 0$  and at least another one in  $0 \leq y \leq +1/2$ . This is the proof of the existence of at least two solutions of the equation (99). But we don't know if there exist solutions in the interval  $y_+ \leq y \leq 1/2$ , and if there exist only one.

The "mean-value theorem" states that if there exist two points  $y_a, y_b$ ,  $y_a < y_b$ , such that  $S(y_{a,b}) = 0$ , then there is, at least, a point  $y_0$ ,  $y_a < y_0 < y_b$ , such that  $S'(y_0) = 0$ . As we have at least two roots of the equation  $S(y, z, a) = 0$ , then, if we find  $y_0$ , we can assert that one root must be a value greater than  $y_0$  (and another one less than  $y_0$ ). Therefore, if  $y_+ \leq y_0$  or  $y_+ \leq y_1$  then we will prove that one single cut point will be outside the hole.

We assert that there is a solution beyond the outer horizon iff.  $y_+ \leq y_{01} = 0$ , that is equivalent to

$$z \leq z_{limit}(a) \equiv \frac{1 + (1 - a^2)^{1/2}}{\frac{1}{2} + (1 - a^2)^{1/2}}. \quad (116)$$

since, according to (115)  $y_{02} \leq y_+$ . Nevertheless, there exist spherical orbits with  $z > z_{limit}$ , so we don't know if in this limiting cases the root of  $S$  could be inside the outer horizon. But this is not possible since  $S(y_+) \leq 0$  and then the root must be outside the horizon (the equality meets in the limit when  $y_+ = 1/2$ ).

### Acknowledgements

We wish to thanks our colleagues Dr. J. Llosa and Dr. C.F. Sopena for their help and useful comments.

## References

- [1] S. Drasco and S.A. Hughes, Phys. Rev. D, **73**, 024027 (2006).
- [2] Y. Mino, Phys. Rev. D, **67**, 084027 (2003).
- [3] N. Sago, T. Tanaka, W. Hirida, K. Gantz and H.Nakano, Prog. Theor. Phys., **115**, 873-907, (2006)
- [4] S. Drasco and S.A. Hughes, Phys. Rev. D, **69**, 044015 (2004).
- [5] W. Schmidt, Class. Quantum Grav., **19** 2743 (2002).
- [6] H. Goldstein, *Classical Mechanics*, (Addison-Wesley, Reading MA, 1980)
- [7] S. Chandrasekhar, *The Mathematical Theory of Black Holes*, (Oxford University Press, Oxford, 1983).
- [8] E. Teo, Gen. Rel. and Grav., **35**, 1909 (2003).
- [9] D.C. Wilkins, Phys. Rev. D, **5**, 814, (1972).
- [10] T. Apostolatos, Phys. Rev. D, **47**, 5376 (1993).
- [11] F.D. Ryan, Phys. Rev. D, **53**, 3064 (1996).
- [12] D. Kennefick and A. Ori, Phys. Rev. D, **53**, 4319, (1996).
- [13] J.M. Bardeen, W.H. Press and S.A. Teukolsky, Ap. J., **178**, 347 (1972).
- [14] D.J. Struik, *Lectures on Classical Differential Geometry*, (Addison-Wesley Publishing Company, Cambridge, Massachusetts, 1961).
- [15] Ch. Misner, K. Thorne, A. Wheeler, *Gravitation*, (W.H. Freeman and Company, San Francisco, 1973)
- [16] J.R. Gair and K. Glampedakis, Phys. Rev. D, **73**, 064037, (2006). gr-qc/0510129v2